EFFECTS OF FIBER ORIENTATION ON MODE I CRACK PROPAGATION IN A MULTIDIRECTIONAL CARBON-EPOXY LAMINATES

M.S. Bin Mohamed Rehan[1,2*], J. Rousseau[1], X.J. Gong[1], S. Fontaine[1] and J.S.M. Ali[2]

[1]*Institut Supérieur de l'Automobile et des Transports, Université de Bourgogne, 58000 Nevers, France*
[2]*Department of Mechanical Engineering, Faculty of Engineering, International Islamic University Malaysia, 50728 Kuala Lumpur, Malaysia*
**Muhammad-Saifuddin.Bin-Mohamed-Rehan@u-bourgogne.fr*

Keywords: Delamination, Fiber orientation, Mode I fracture, Multidirectional laminates.

Abstract
The influence of fiber orientation on mode I crack propagation in multidirectional carbon-epoxy laminates was investigated. The double cantilever beam (DCB) specimens are designed so as to obtain an uncoupled quasi-isotropic and quasi-homogeneous elastic behavior. Resistance to crack initiation and propagation, characterized by critical strain energy release rate, G_{IC} and R-curve, respectively, is investigated. Measured G_{IC} appear to change with the orientation of plies on each side of the crack interface. More pronounced differences are observed on R-curves, as the ply orientations at the interface lead to different crack propagation mechanisms. Observation on crack front shape by ultrasonic scanning shows an influence of the fiber orientation on each side of the crack.

1 Introduction
Efforts in characterization of delamination resistance, in particular mode I fracture, have led to the standardization of the double cantilever beam (DCB) test for measuring the critical strain energy release rate, G_{IC}, of unidirectional (UD) laminates [1-3]. Even though such specimens are quite convenient for testing purposes, most applications involve multidirectional (MD) laminates, where delamination occurs between layers of different fiber orientations. Hence obtaining G_{IC} values of MD specimens is of great importance for the development of accurate fracture criteria.

Some studies have concluded that the measured mode I toughness in term of G_{IC} is practically independent of the fiber orientation of the delaminating interface [4], while significant variation of G_{IC} was observed in other studies [5,6]. A study even indicated that the values of G_{IC} are affected not only by the fiber orientation of the adjacent plies, but also by the fiber orientation of the sub-adjacent plies [7].

The present work is a continuation of the study reported in Mohamed Rehan et. al. [8]. Specimens having special stacking sequences are tested and analyzed in order to better understand the effect of fiber orientation of the adjacent plies on the behavior of crack initiation and propagation under mode I loading.

2 Material and testing methods

2.1 Design of MD DCB specimen

The MD specimens used in the DCB delamination tests have an initial crack at mid-thickness that separates the whole laminate at one end into two sub-laminates (two arms). The stacking sequences of the specimens have been designed so as to allow various combinations of fiber orientation of adjacent and sub-adjacent plies without any change of the elastic behavior of the specimens. Moreover, the laminate as well as each arm possess the same stiffness A_{ij}, B_{ij} and D_{ij}, where uncoupled ($B_{ij} = 0$, $A_{16} = A_{26} = D_{16} = D_{26} = 0$) quasi-isotropic and quasi-homogeneous ($A_{ij}^* \equiv D_{ij}^*$) (QIQH) elastic behavior has been imposed.

The 24-ply QIQH laminates described by Galliot et. al. [9] have been used for each arm of the specimens, resulting in a 48-ply QIQH laminate. Five stacking sequences, as shown in Table 1, and thus five different crack interfaces, are studied. For convenience, the specimens are identified by the orientation of the first two plies adjacent to the crack, with "//" indicating the crack. All specimens have the same ABD matrix.

Specimen	Stacking sequence
(90/0//0/90)	[90/0/-45/45/-45/45/0/45/90/-45/90/0/90/0/45/0/-45/90/-45/45/-45/45/90/0]sym
(45/0//0/45)	[45/0/90/-45/90/-45/0/-45/45/90/45/0/45/0/-45/0/90/45/90/-45/90/-45/45/0]sym
(-45/45//45/-45)	[-45/45/0/90/0/90/45/90/-45/0/-45/45/-45/45/90/45/0/-45/0/90/0/90/-45/45]sym
(90/45//45/90)	[90/45/-45/0/-45/0/45/0/90/-45/90/45/90/45/0/45/-45/90/-45/0/-45/0/90/45]sym
(0/90//90/0)	[0/90/45/-45/45/-45/90/-45/0/45/0/90/0/90/-45/90/45/0/45/-45/45/-45/0/90]sym

Table 1. Stacking sequences studied.

2.2 Material and preparation of specimen

Double cantilever beam (DCB) specimens are produced from 150 g/m² carbon/epoxy prepregs from Structil (ref. CTE1 15). The 48-ply DCB specimens have 15 µm thick polyester film embedded as the crack starter at mid-thickness of the specimen. Laminates are cured in a hot press at 125 °C and 3.9 bar for 100 minutes. The laminates are then cut into specimens with the desired geometries. Similar specimen geometries are ensured to isolate the ply orientations as the only factor affecting the observed behavior of crack initiation and propagation. The nominal values of specimen initial crack length, width, and thickness are 70 mm, 20 mm and 7.0 mm, respectively. The measured specimen dimensions are as shown in Table 2.

Specimen	Width, b (mm)	Thickness, 2h (mm)	Initial crack length, a_o (mm)
(90/0//0/90)	20.28 (0.90)	6.94 (1.07)	70.02 (0.42)
(45/0//0/45)	20.32 (0.71)	7.05 (1.49)	70.11 (1.08)
(-45/45//45/-45)	19.89 (0.67)	7.05 (0.98)	70.16 (0.97)
(90/45//45/90)	20.26 (0.76)	7.06 (0.78)	70.34 (0.94)
(0/90//90/0)	20.19 (1.16)	7.01 (1.77)	69.45 (1.60)

Table 2. Mean values of specimen dimensions (coefficient of variation (%) in brackets).

2.3 Testing methods

The DCB specimens are loaded on a static tensile machine at room temperature with constant crosshead speed of 0.5 mm/min. The load-displacement data are recorded during the test. G_{IC} and R-curves are then obtained from these recorded data.

Ultrasonic scanning was performed on specimens of each stacking sequence. C-scan image is acquired before loading, showing the initial crack front. The specimen is loaded until the initiation of the crack propagation. The test is stopped to remove the specimen so as to acquire a new C-scan image. The specimen is then loaded again until the crack propagates for a few millimeters. These steps are repeated several times for each specimen. The C-scan images are compiled and analyzed to extract the crack front shape and position at each interval. Figure 1 shows a sample of a C-scan image of the delamination in the DCB specimen from which the crack front line is extracted.

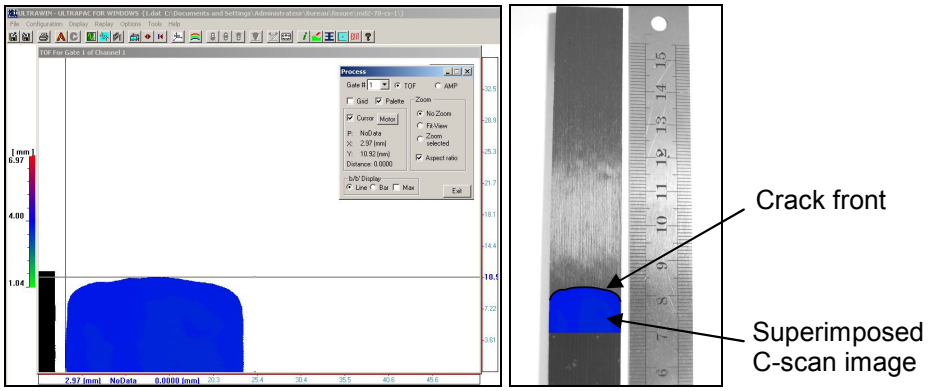

Figure 1. A crack front shape obtained by C-scan.

3 Experimental results and analysis

3.1 Data reduction methods

In this study, compliance calibration method associated with Berry's model is used for G_{IC} calculations:

$$G_{IC} = \frac{nP_C\delta_C}{2ab} \text{ with Berry's compliance calibration } C = \alpha a^n \tag{1}$$

where specimen compliance C is the ratio of the load point displacement δ to the applied load P; P_c and δ_c are the critical load and the displacement at crack initiation, respectively; b is the specimen width and a is the initial crack length.

The effective crack length, a_i, and strain energy release rate, G_{Ii}, for the crack propagation is then calculated as:

$$a_i = \left(\frac{C_i}{\alpha}\right)^{1/n} \tag{2}$$

$$G_{Ii} = \frac{P_i^2}{2b}\alpha n a_i^{n-1} \tag{3}$$

To calculate the modulus of elasticity of laminate, the following equation based on beam theory is used:

$$E = \frac{8a^3}{bh^3C} \tag{4}$$

where *b* is the specimen width and *h* is the thickness of each arm.

3.2 Load-displacement curves and observations during the tests
The load-displacement plots obtained from the DCB tests are shown in Figure 2.

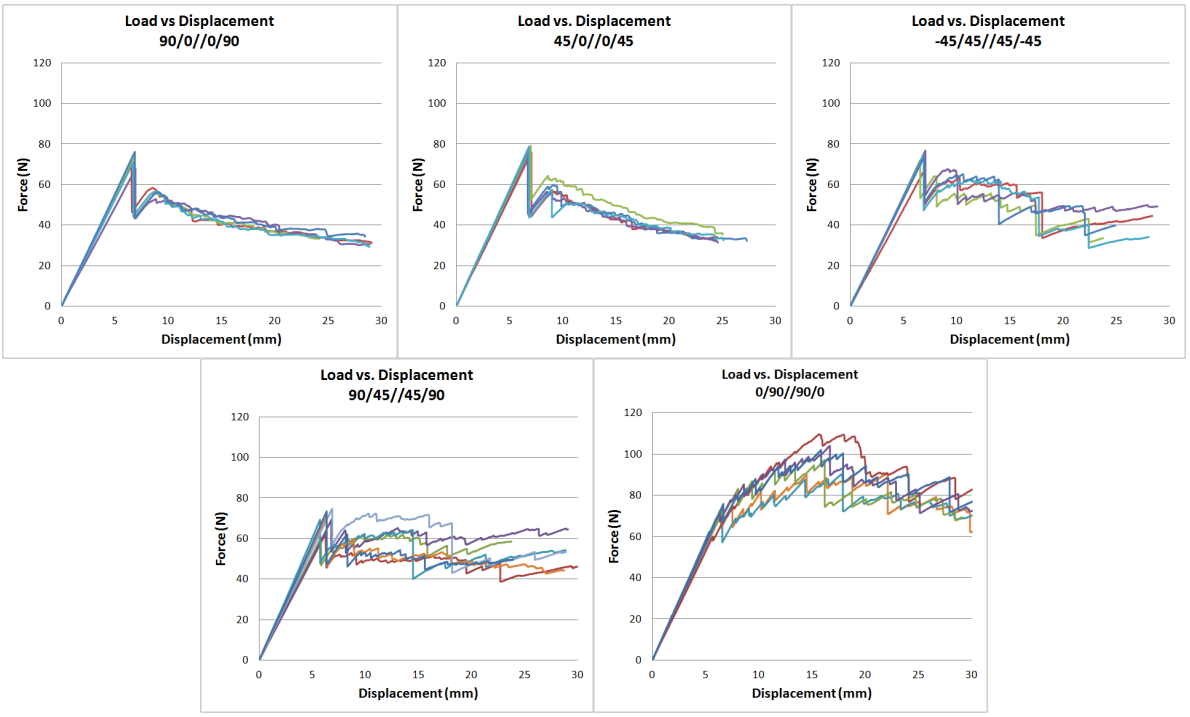

Figure 2. Load-displacement plots for specimens tested.

All the specimens exhibit unstable crack propagation behavior at the crack initiation, in the form of a sudden jump in the crack extension, accompanied by an audible sound. This phenomenon appears in the load-displacement curves as a sudden drop in the applied load. Similar observation has been reported in the literature, it can be attributed to the influence of the starter crack [10]. The curves show that the magnitude of this drop in load increases with the decrease of the angle of fiber orientation of adjacent plies from 90° to 0°. The angle θ between the direction of crack propagation and fiber orientation appears to be a major hurdle for this unstable extension of the crack.

After the crack initiation, the crack growth is rather stable, but with local instability periodically more or less marked. The fluctuations due to drops in the load become more pronounced for higher θ. Moreover, the variation of the load as the crack grows depends not only on the fiber orientation of adjacent plies, but also on that of the sub-adjacent plies.

3.3 Elastic properties
As one of the objectives of the specimen design is to isolate the ply orientation as the only factor influencing crack behavior, it is important to evaluate whether this objective is achieved. Table 3 presents the mean values of normalized compliance and modulus of elasticity calculated by using equation (4). The coefficients of variation are measured from a set of five samples for each staking sequence. It can be observed that all specimens with different stacking sequences have practically the same compliance and modulus of elasticity.

Specimen	Normalized compliance, C (10^{-6} m/N)	Modulus of elasticity, E (GPa)	Critical strain energy release rate, G_{IC} (N/m)
(90/0//0/90)	92.74 (2.28)	34.52 (2.28)	490.31 (10.51)
(45/0//0/45)	92.64 (1.43)	34.55 (1.43)	542.07 (3.36)
(-45/45//45/-45)	95.51 (2.76)	33.52 (2.80)	507.26 (10.05)
(90/45//45/90)	95.35 (2.03)	33.57 (2.05)	454.36 (14.13)
(0/90//90/0)	92.47 (2.20)	34.62 (2.23)	439.76 (16.55)

Table 3. Mean values of normalized compliance, modulus of elasticity, and critical strain energy release rate for corresponding specimen (coefficient of variation (%) in brackets).

3.4 Comparison of measured G_{IC} on five laminates tested

The values of G_{IC} measured on the specimens tested are also presented in Table 3. The high coefficients of variation illustrate a dispersion of these values for each corresponding specimen set. Between the five laminates, the maximum value of G_{IC} is about 23% higher than the minimum value. Different ply orientation of subsequent ply seems to affect the mean G_{IC} values for both 0° and 45° interfaces, though the high dispersion does not allow this observation to be conclusive enough.

3.5 R-curve

The R-curves for the propagation after crack initiation are presented in Figure 3 in the form of effective G_I against crack extension. The curves are clearly different for different crack interfaces. In each plot, the sudden jump at crack initiation can be identified by the sudden big increase in crack extension accompanied by a drop in G_I. Afterwards, the trends of the curve differ based on the ply orientation at the crack interface.

For 0°//0° interfaces, no significant effect is observed when the fiber orientation of sub-adjacent plies change from 45° to 90°. Effective G_I stabilizes at around 400 N/m, and the fluctuation is small. This is in line with the experimental observations that very little fiber bridging occurred during the tests.

For 45°//45° interfaces, after the unstable crack propagation at crack initiation, the effective G_I increases with a similar rate for the two laminates. However, for (-45/45//45/-45) laminates, there is a tendency for the effective G_I to suddenly drop back again to a value around 400 N/m, before it increases again with crack extension. Herein, the bridging that builds up tend to break at a certain point, which cause the G_I value to instantaneously drop, before increasing again as fiber bridging intensify.

As regards the (90/45//45/90) laminates, after the crack has propagated a certain length, effective G_I increases with a higher slope. This phenomenon is due to the crack migration into the subsequent interface, where the resistance to crack propagating at the 90° ply is higher compared to that of the original interface of 45°//45°. The migration of the crack from 45° interface to the 90° ply is illustrated by the crack surface of the specimen shown in Figure 4. This leads to a different propagation behavior after this migration of the crack.

For the specimens with 90°//90° interface, the jump at crack initiation is smaller, as indicated for the load-displacement curves. In this case, G_I increases until it stabilizes after around 20 mm of crack extension.

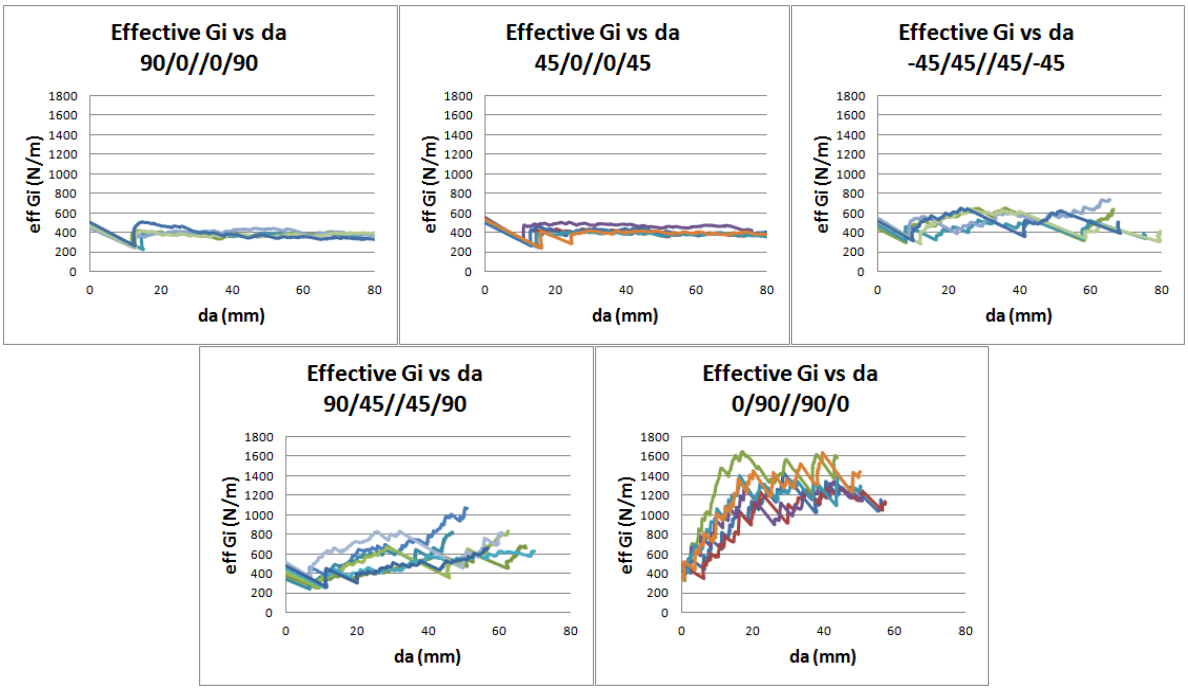

Figure 3. R-curves for five laminates tested.

3.6 Fracture surfaces

The fracture surfaces of the tested specimens are shown in Figure 4. Both laminates with 0°//0° interfaces have a macroscopically smooth surface, with very little sign of fiber bridging. This explains the quasi-constant resistance to crack propagation for the two laminates having 0°//0° interfaces. For other specimens, rough surfaces are observed, indicating fiber bridging phenomenon. For specimen (45/0//0/45), crack propagates within the 45°//45° interface, while for specimen (90/45//45/90), the crack tends to migrate to the 45°//90° interface. Two samples from specimen (90/45//45/90) are shown in Figure 4, illustrating different locations of crack migration observed during the tests. The curves in Figure 3 that have earlier increase in slope correspond to the specimens that underwent earlier crack migration. For specimen (0/90//90/0), very rough surfaces are observed, but no crack migration is observed for this laminate. These observations highlight the possibility of the fiber orientation of sub-adjacent plies being an important factor in the migration of the crack.

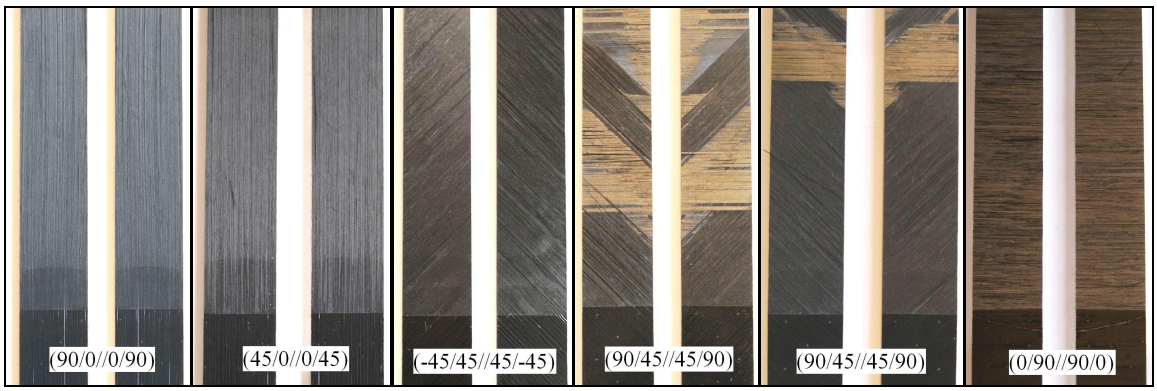

Figure 4. Fracture surfaces (both arms of a specimen of each laminate).

3.7 Crack front shape

The lines corresponding to the crack front at different intervals are extracted from the C-scan images and plotted on the fractured specimen pictures (as illustrated in Figure 1). Due to the

crack extension "jumps" that occur throughout most of the tests, alongside with other technical factors, the crack front scans could not be obtained at the same intervals for all specimens. Moreover, the diffraction of the ultrasound wave near the edges of the laminate did not allow for determination of the precise shape of the crack front in these zones. Only the inner part of the various crack fronts is plotted in Figure 5.

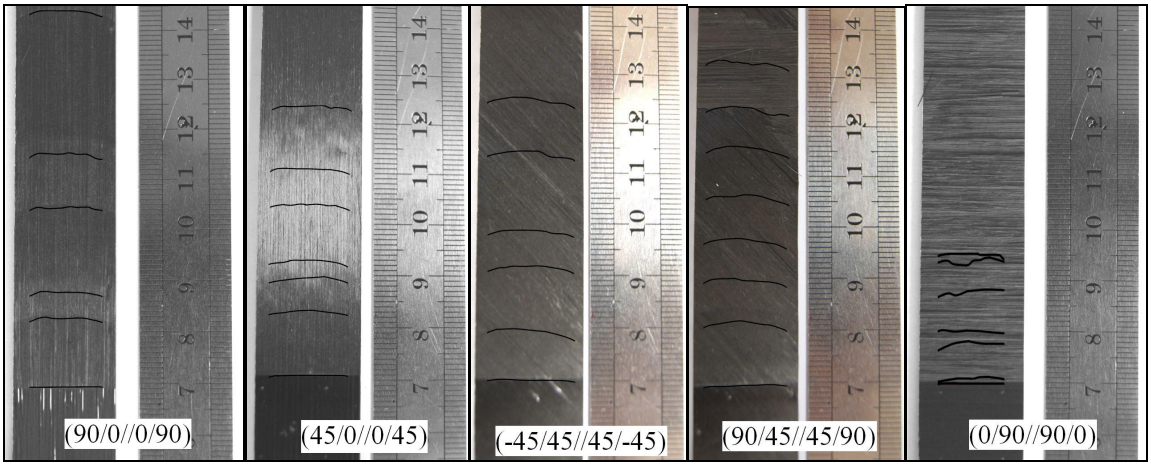

Figure 5. Samples of crack front extracted from C-scan on specimens tested.

For all specimens shown, the second crack front line after the initial crack is obtained immediately after the crack extension jump that occurred at crack initiation. The initial jump for 0°//0° and 45°//45° interfaces covers up to 13 mm of crack length. This is observed for all specimens (with mentioned interfaces) tested in this study. This implies that it is impossible to follow the use of load induced precracking steps suggested in ASTM 5528-94a [1], as it specifies to stop loading for the pre-crack after delamination growth of 3-5 mm.

Another issue in using the load induced precracking is that not only the initial crack front position after precracking (or the precracking length) is not going to be the same for all specimens, but the crack front shape would also not be the same between specimens. Such factors can come into picture if the objective of a study is to perform a comparison between different specimens.

The crack front has a symmetrical shape for the specimens with 0°//0° crack interface, while it tend to be more slanted for specimens with 45°//45° interface. This indicates that even though the specimens are globally the same, the crack front shape is actually affected by the local orientations.

4 Conclusions

DCB test have been performed on specimens having five different stacking sequences, all of which being uncoupled quasi-isotropic and quasi-homogeneous multidirectional carbon-epoxy laminates. Comparison of measured compliance and modulus of elasticity confirmed that the specimens from the five different layups have the same elastic properties. However, certain differences in the mean values of critical energy release rate G_{IC} has been revealed between the five crack interfaces tested. But the dispersion of the values for most specimens is too high for it to be conclusive. As for the crack propagation, the dependency of R-curves on crack interface is more remarkable. Specimens with 0°//0° crack interface produced no toughening effect as no significant fiber bridging occurred during the test. Fiber bridging was observed for specimens with 45°//45° crack interface, leading to the increase of the resistance to crack growth. For specimens with 90°//90° crack interface, R-curves with much higher

slope are obtained, as the crack path has to go around the fibers that are perpendicular to the propagation direction. The observation of the R-curves and fracture surfaces indicates that the crack mechanism, and hence the crack behavior, is directly affected by ply orientation of not only the adjacent ply, but also the sub-adjacent plies. Finally, the change of crack front shapes seems dependent of local fiber orientation of adjacent plies.

References

[1] ASTM 5528-94a. *Standard test method for mode I interlaminar fracture toughness of unidirectional fiber-reinforced polymer matrix composites* (2000).

[2] ISO 15024:2001. *Fibre-reinforced plastic composites – Determination of mode I interlaminar fracture toughness, G_{Ic}, for unidirectionally reinforced materials* (2001).

[3] Brunner A.J., Blackman B.R.K., Davies P. A status report on delamination resistance testing of polymer-matrix composites. *Engineering Fracture Mechanics*, **Volume 75(9)**, pp. 2779-2794 (2008).

[4] Pereira A.B., de Morais A.B. Mode I interlaminar fracture of carbon/epoxy multidirectional laminates. *Composites Science and Technology*, **Volume 64(13-14)**, pp. 2261-2270 (2004).

[5] Hiley M.J. *Delamination between multi-directional ply interfaces in carbon-epoxy composites under static and fatigue loading* in "European Structural Integrity Society", edited by Williams J.G. and Pavan A. Elsavier, **Volume 27**, pp. 61-72 (2000).

[6] Benzeggagh M.L., Gong X.J., Laksimi A., Roelandt J.M. On the test of mode I delamination and the importance of stratification. *Polymer Engineering and Science*, **Volume 31(17)**, pp. 1286-1292 (1991).

[7] Gong X.J., Hurez A., Verchery G. On the determination of delamination toughness by using multidirectional DCB specimens. *Polymer Testing*, **Volume 29(6)**, pp. 658-666 (2010).

[8] Mohamed Rehan M.S., Rousseau J., Gong X.J., Guillaumat L., Ali J.S.M. Effects of fiber orientation of adjacent plies on the mode I crack propagation in a carbon-epoxy laminates. *Procedia Engineering*, **Volume 10**, pp. 3179-3184 (2011).

[9] Galliot C., Rousseau J., Valot E., Verchery G. *Influence of stacking sequence on the strength of composite bonded joints* in Proceeding of 16th International Conference on Composite Materials, Kyoto, Japan, (2007).

[10] Schön J., Nyman T., Blom A., Ansell H. A numerical and experimental investigation of delamination behavior in the DCB specimen. *Composites Science and Technology*, **Volume 60**, pp. 173-184 (2000).